

Analysis of $\eta\pi^0$ system with the decay $\eta \rightarrow \pi^+\pi^-\pi^0$. Stage 2.

V.L.Korotkikh, L.V. Malinina

24 December 2004

Scobeltsyn Institute of Nuclear Physics
Moscow State University, 119992 Moscow, Russia

Version 1

Abstract

The exclusive reaction $\pi^-p \rightarrow \eta\pi^0n$, $\eta \rightarrow \pi^+\pi^-\pi^0$, $\pi^0 \rightarrow 2\gamma$ at 18 GeV/c has been studied. A partial wave analysis has been performed on a sample of 23492 $\eta\pi^0n$ events. A mass dependent fit of the P_+ and D_+ waves and their relative phase gives a candidate of neutral exotic $J^{PC} = 1^{-+}$ state production.

Introduction

In our previous works we reported evidence for an exotic $J^{PC} = 1^{-+}(1400)$ resonance state in the reaction $\pi^-p \rightarrow \eta\pi^-p$, $\eta \rightarrow 2\gamma$. The Crystal Barrel experiment confirmed this result for $\eta\pi^-$ system in the reaction with antiprotons stopped in liquid deuterium, $\bar{p}n \rightarrow \pi^-\pi^0\eta$. Later this group presented evidence for production of the exotic 1^{-+} resonance in the $\eta\pi^0$ system in data on $\bar{p}p$ annihilation at rest into $\pi^0\pi^0\eta$ with $M = (1360 \pm 25)$ MeV/c² and $\Gamma = (220 \pm 90)$ MeV/c².

We have studied the reaction $\pi^-p \rightarrow \eta\pi^0n$, $\eta \rightarrow \pi^+\pi^-\pi^0$, $\pi^0 \rightarrow 2\gamma$ at 18 GeV/c. The important and obvious characteristic of the $\eta\pi^0$ system unlike $\eta\pi^-$ system is that C -parity is a good quantum number. Thus it is possible to study the exotic (non $q\bar{q}$) state with quantum numbers $J^{PC} = 1^{-+}$. The other distinguishing feature of the charge exchange reaction $\pi^-p \rightarrow \eta\pi^0n$ is that, unlike $\eta\pi^-p$ production, the production mechanism cannot involve the exchange of an $I=0$ system and thus pomeron exchange is ruled out.

Finally, it is important to note that, from the experimental point of view, in the reaction $\pi^- p \rightarrow \pi^+ \pi^- 4\gamma n$ we can define the interaction point by the charged tracks and convince ourself that the event is in the target region. This is not possible in the all neutral final state when the η decays to 2 photons.

The data for this analysis was obtained in the E852 experiment at the Alternating Gradient Synchrotron (BNL USA) during 1995. Using an 18 GeV/c π^- beam interacting with liquid hydrogen targe, a total of 750 million triggers were acquired of which 108 million were of a type designed to enrich the exclusive final state events $\pi^- p \rightarrow \pi^+ \pi^- 4\gamma n$. A total 6 million events of this type were fully reconstructed. The data were kinematically fitted to select events consistent with an $\pi^- \pi^+ \pi^0 \pi^0 n$ hypothesis. 3973000 events were fully reconstructed, after mass cut $m(\pi^- \pi^+ \pi^0) > 0.65 GeV$ we have 85228 events and after ellips cut (where the drift chamber efficiency was low, run 1995 year) 74549 events of $\pi^- \pi^+ \pi^0 \pi^0 n$.

Then the data were kinematically fitted to select 31679 events consistent with an $\eta \pi^0 n$ hypothesis. Requiring a minimum acceptable confidence level of 1% for this hypothesis, a total of 23492 $\eta \pi^0 n$ events remained for the partial wave analysis (PWA).

1 Cut of mass

The cut mass $m(\pi^0\pi^+\pi^-) > 0.65\text{GeV}$ is presented on Fig. 1.

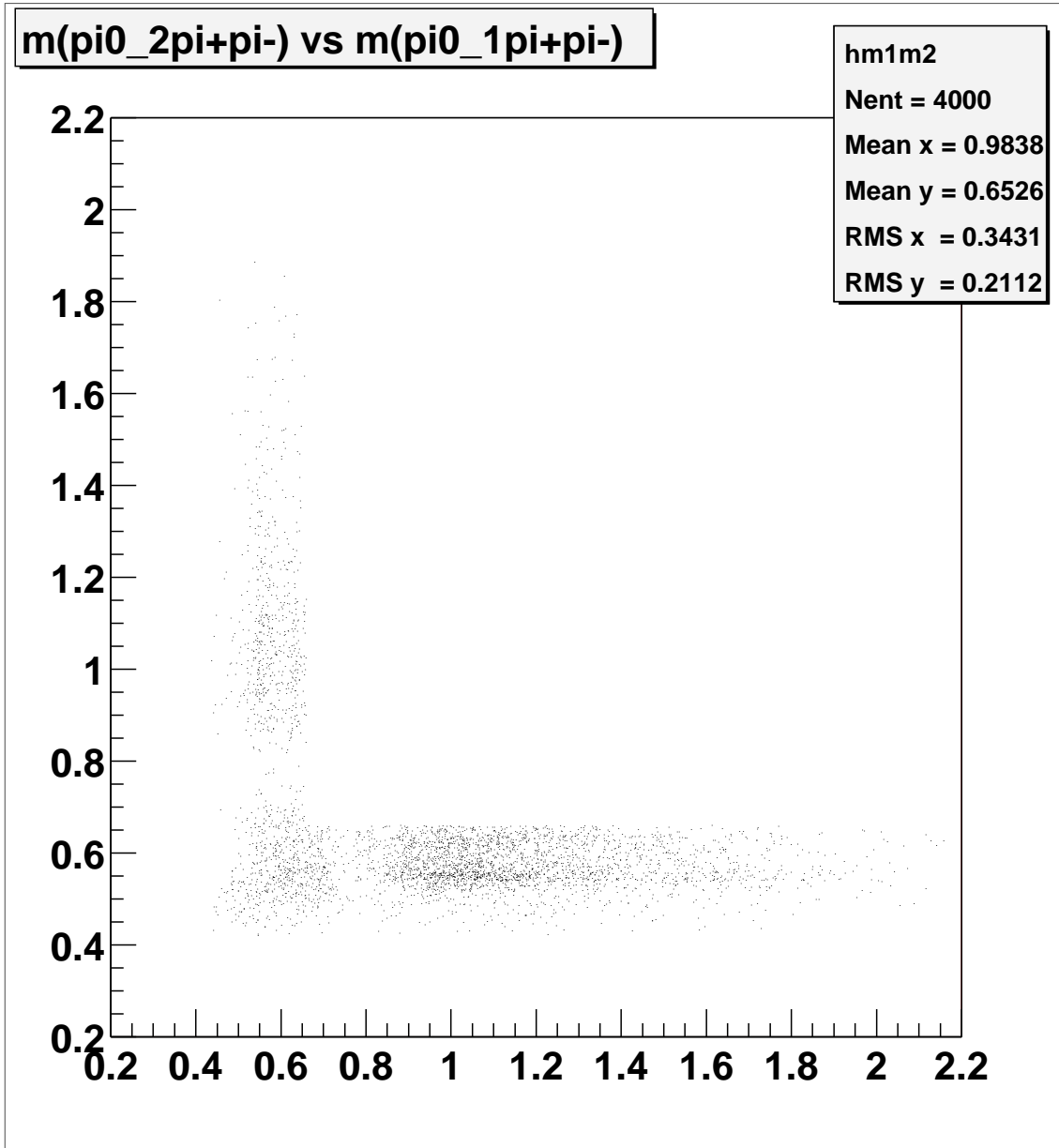


Figure 1: Sample of 4000 events, two demension plot of mass($\pi^0\pi^+\pi^-$) distribution, mass cut $m(\pi^0\pi^+\pi^-) > 0.65\text{GeV}$

Distributions of 4π -system are shown on Fig. 2 and on Fig. 2 before and after mass cut.

2 Background of $\eta\pi^0$ distribution

Selection of the side bands near η signal is on Fig. 4

Calculated background and a ratio Bcgr/Data are on Fig. 5 and Fig. 6

3 Distributions for $\eta\pi^0$ system

We demonstrate the results on Fig. 7.

The dependence of $\eta\pi^0$ system mass shows two well-defined peaks at 1.0 and 1.3 MeV/c². We fit the t' -dependence of the acceptance corrected data for all masses using the expression

$$N(t') = n_1 e^{-b_1|t'|} + n_2 |t'| e^{-b_2|t'|}$$

and find the values of parameters

$$b_1 = (5.5 \pm 1.6)(\text{GeV}/c)^2, \quad b_2 = (5.40 \pm 0.04)(\text{GeV}/c)^2.$$

4 PWA and Mass Dependent Fit

The PWA was performed on the sample of 23492 $\eta\pi^0 n$ events (note that for $\eta\pi^- p$ events [1] there were 47200 events) for $0.78 < M(\eta\pi^0) < 1.72$ GeV/c² and $0.1 < |t'| < 1.0$ (GeV/c)² in $\Delta M = 40$ MeV/c² mass bins. The PWA has been done using 7 amplitudes: S_0, P_0, P_-, D_0, D_- (unnatural parity exchange, UNPE) and P_+, D_+ (natural parity exchange).

The D_+ and P_+ waves are the main contributions to the total intensity. The ratio of P_+ and D_+ wave intensities is greater (about 20%) than for the $\eta\pi^-$ system [1]. The same ratio is observed for the $\eta\pi^0$ system in the GAMS analysis. The contribution from the UNPE waves is smaller except for the D_0 wave (about 20%), but the spread of the UNPE ambiguous solutions is larger than for the $\eta\pi^-$ system. For this reason, the shape of the P_+ intensity distribution depends strongly on solution. The phase motion between the P_+ and the D_+ waves is very similar to that in the $\eta\pi^-$ system [1] as well as that of the $\eta\pi^0$ system of GAMS. The goodness-of-fit for the PWA is good. The comparison of the data moments $H(LM)$, ($L \leq 2, M \leq 2$) and their prediction from the PWA gives $\chi^2/dof = 0.18$.

Results of PWA are presented on Fig. 8 and Fig. 9.

We simultaneously fit the intensities of the D_+ and P_+ waves and their relative phase in the region $1.02 < M(\eta\pi^0) < 1.74$ MeV/c². See Fig. 10. The central values for the intensities and phases are taken from the PWA as the average values of the ambiguous solutions. The errors are calculated from the average error matrix. The mass dependent fit includes a Breit-Wigner (BW) amplitude for the D_+ wave with a second order polynomial background; a BW amplitude for the P_+ wave (resonant hypothesis) and a mass-independent production phase. For the nonresonant hypothesis we used a Gaussian intensity distribution for the P_+ wave and a linear mass dependence for the production phase.

The result of the fit with the resonant hypothesis ($\chi^2/dof = 1.18$) is in shown in Fig. 10. There is no need to introduce a mass dependence for the production phase in the resonant hypothesis.

Shown are the fitted intensity distributions for $D_+(2^{++})$ and $P_+(1^{-+})$ waves (top left and top right) and their phase difference (left lower figure). The lines on the right lower figure show the fitted BW phase of the 2^{++} state (strong motion), the 1^{-+} state (weak motion) and the mass independent production phase.

The parameters of the fitted BW amplitudes for the 2^{++} state (a_2^0 meson)

are

$$M(a_2^0) = (1330 \pm 2_{-56}^{+24}) \text{ MeV}/c^2,$$

$$\Gamma(a_2^0) = (85 \pm 3_{-56}^{+140}) \text{ MeV}/c^2,$$

and for the exotic 1^{-+} state (π_1^0 meson)

$$M(\pi_1^0) = (1326 \pm 24_{-50}^{+70}) \text{ MeV}/c^2,$$

$$\Gamma(\pi_1^0) = (470 \pm 81_{-126}^{+34}) \text{ MeV}/c^2.$$

The systematic errors for the mass and width are taken from the range of ambiguous solutions.

Fig. 10.

5 Final remarks

The work on the selection of physical solution between the ambiguous solution is in progres.

Supporting materials are in web site

</home/lemond/e852/WWW/secure/analysis/1995/korotkih>

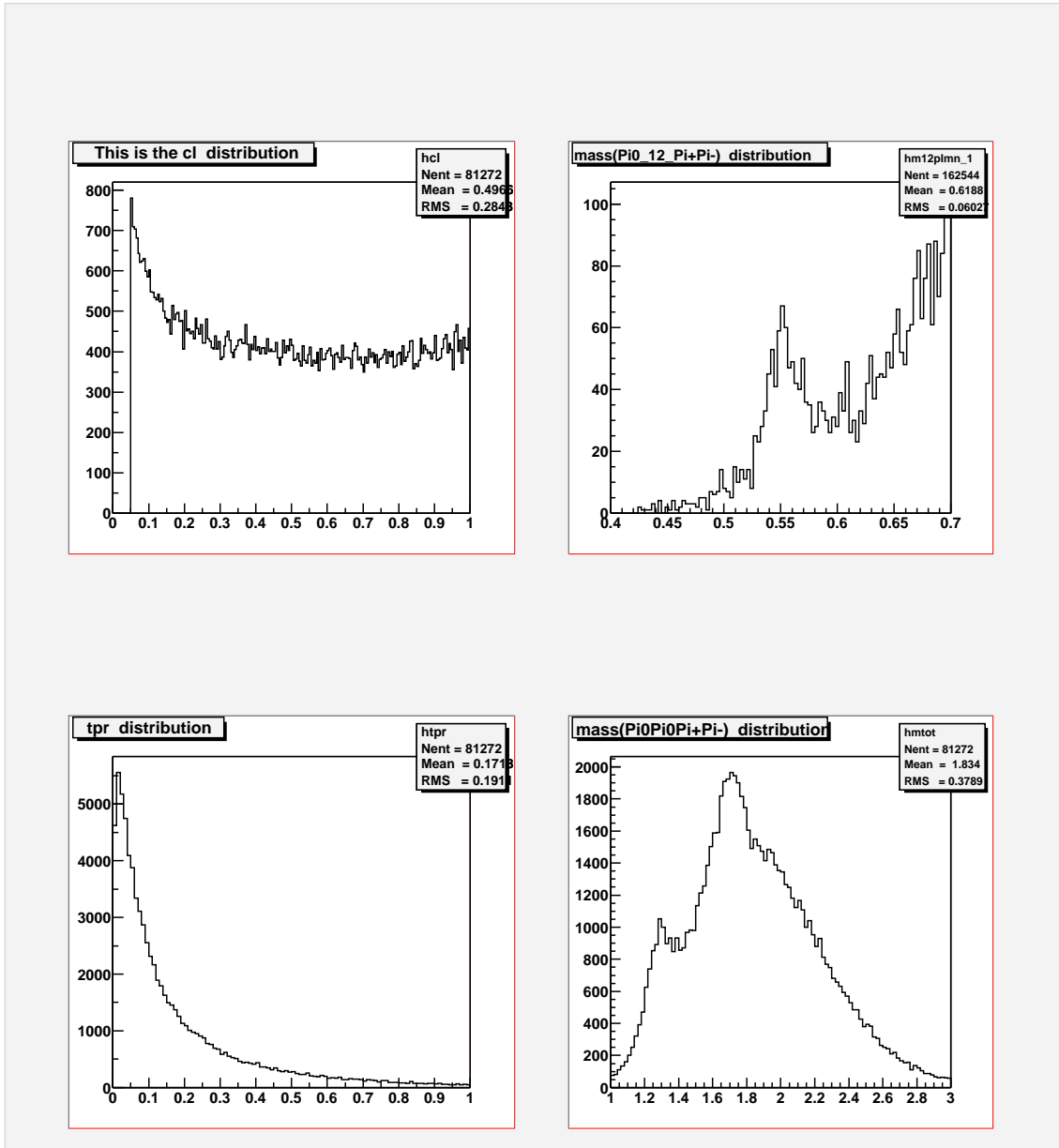


Figure 2: Distributions without mass cut, a) cl - distribution, b) $\text{mass}(\pi^0\pi^+\pi^-)$ distribution, c) t' - distribution, d) $\text{mass}(\pi^0\pi^0\pi^+\pi^-)$ distribution

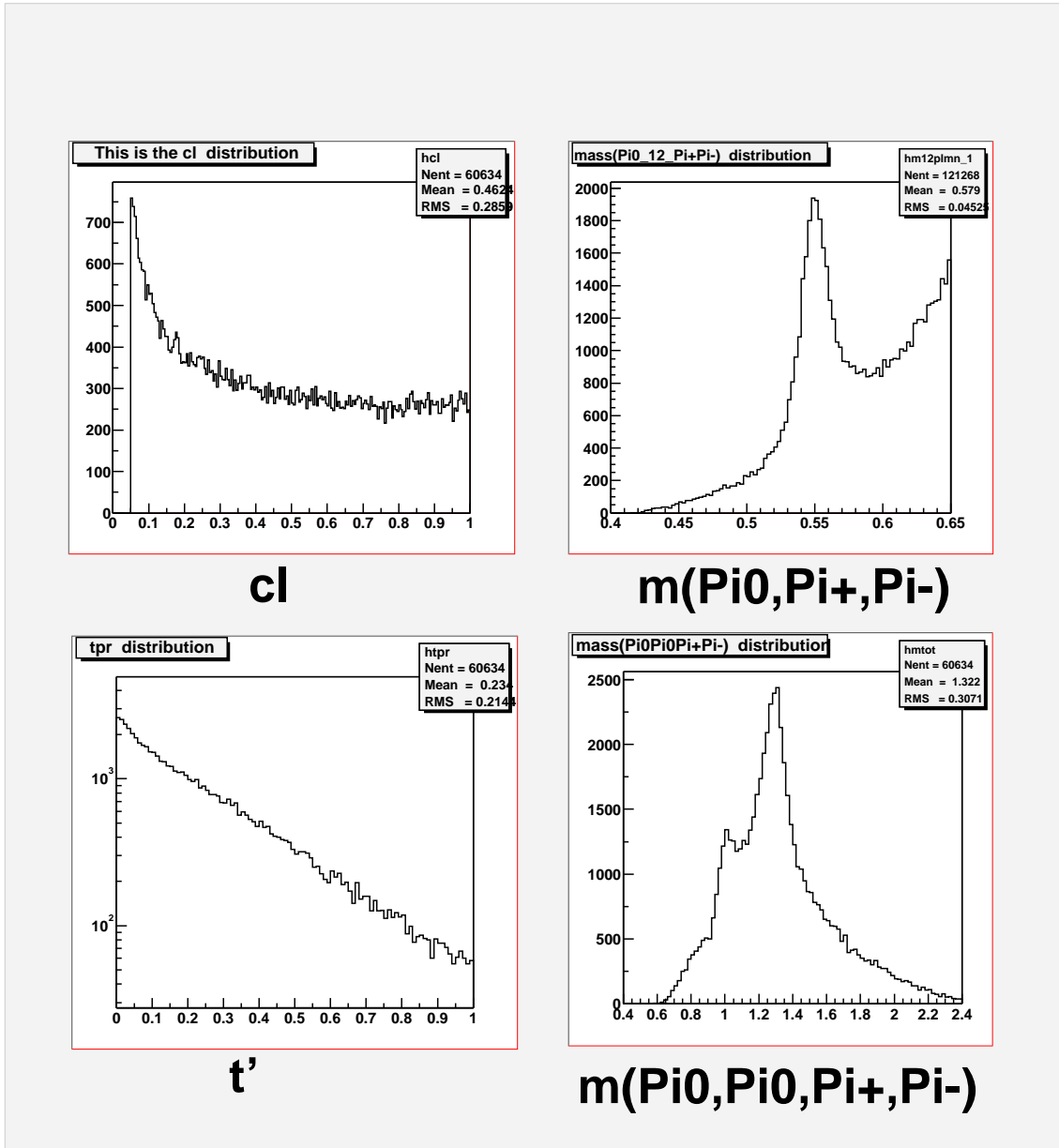


Figure 3: 85228 events, after mass cut, sample 10K events, a) cl - distribution, b) $mass(\pi^0\pi^+\pi^-)$ distribution, c) t' - distribution, d) $mass(\pi^0\pi^0\pi^+\pi^-)$ distribution

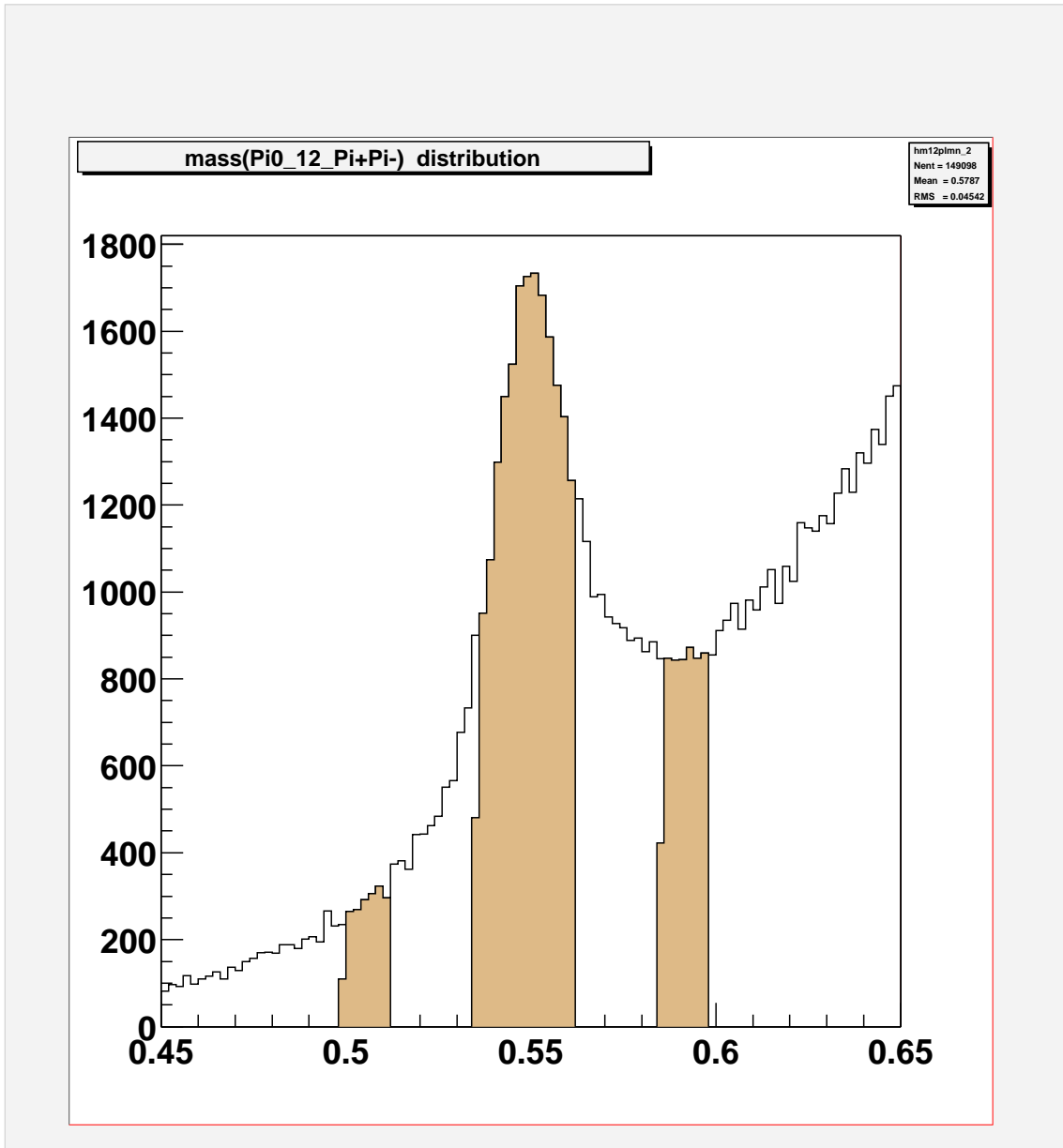


Figure 4: Selection of side bands in the $\pi^0\pi^+\pi^-$ distribution

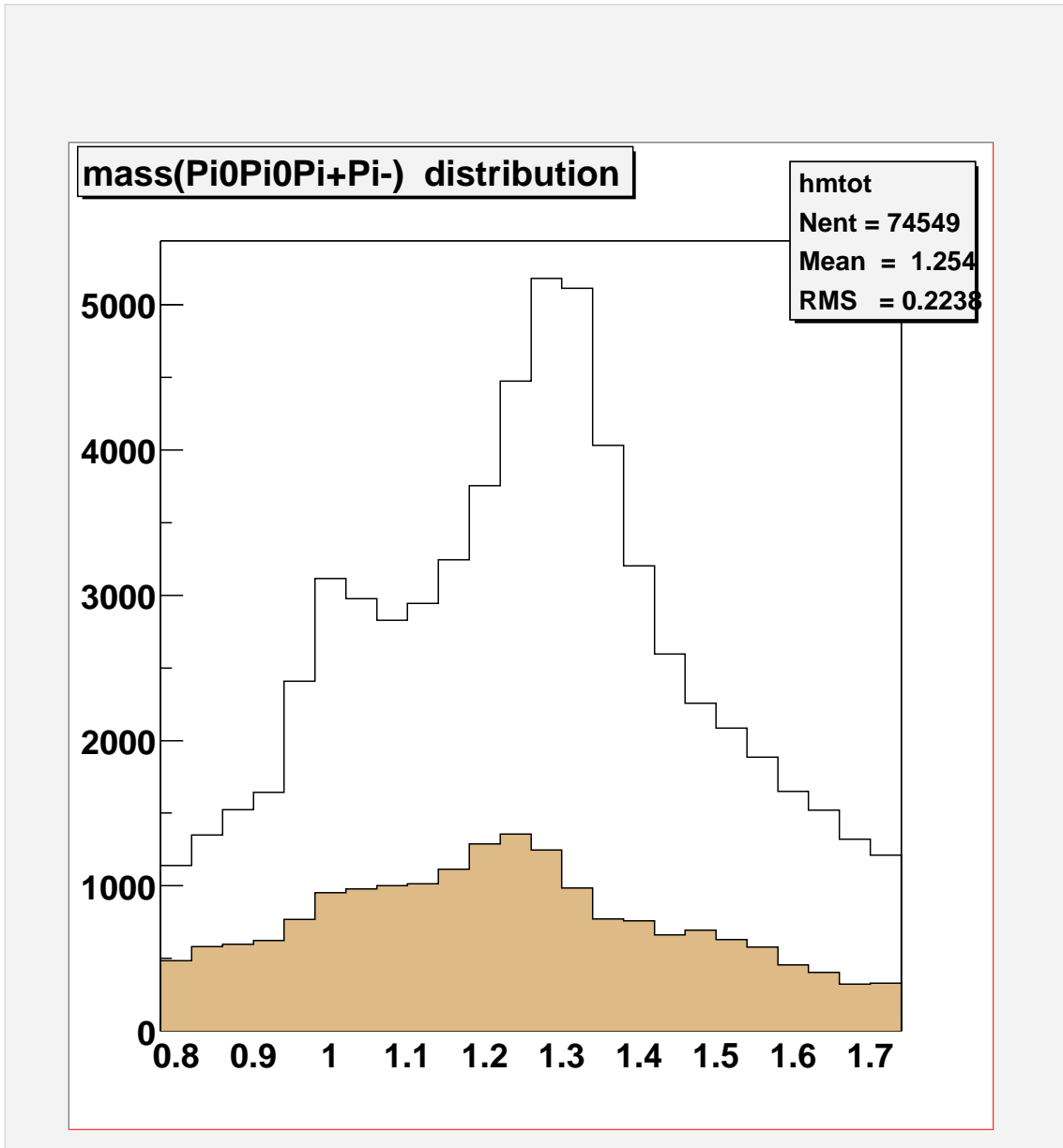


Figure 5: Data and background in the $\pi^0\pi^0\pi^+\pi^-$ distribution

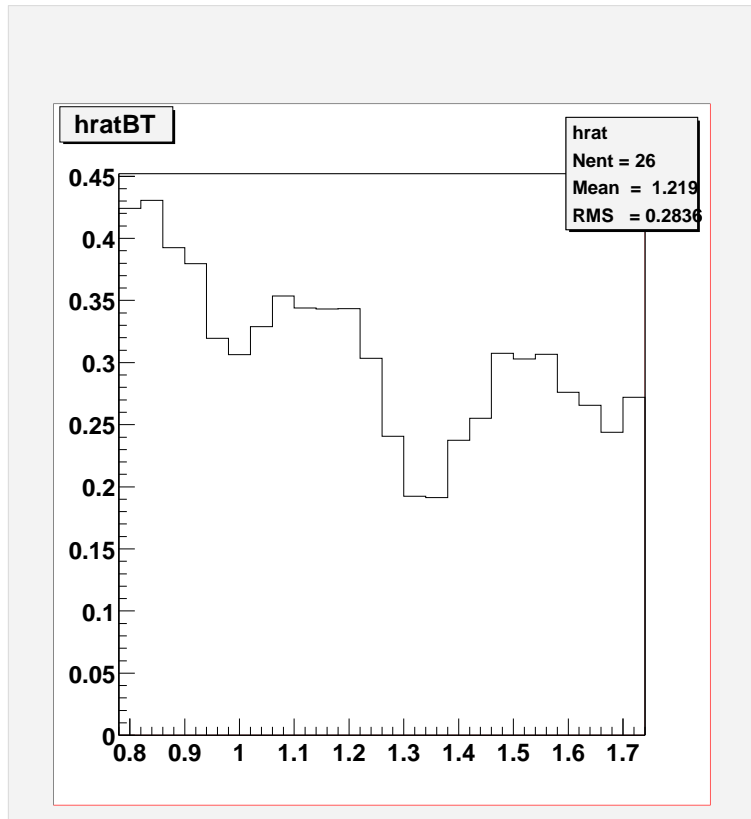


Figure 6: Ratio Bcgr/Data in the $\pi^0\pi^0\pi^+\pi^-$ distribution

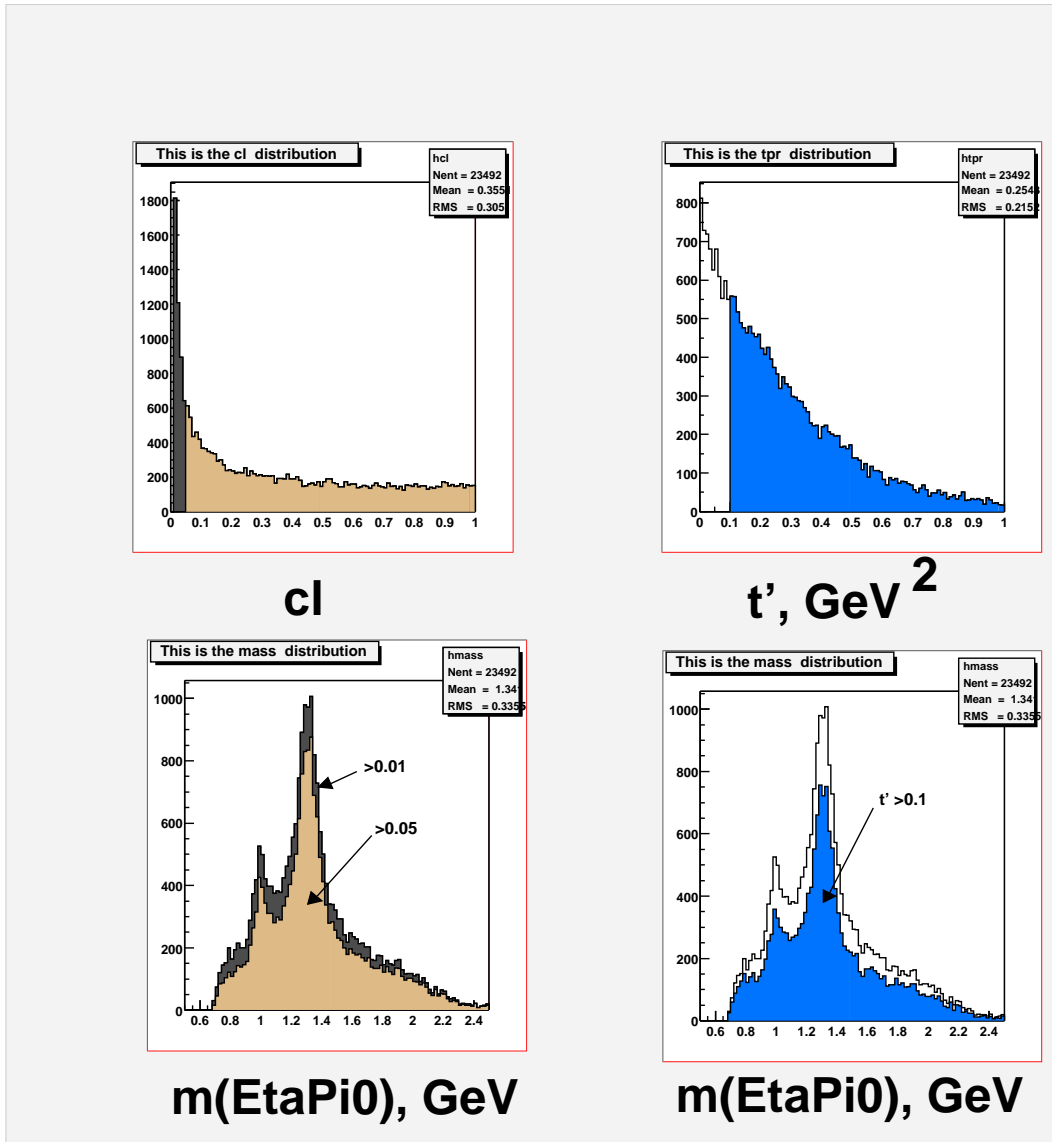


Figure 7: 23492 events after SQUAW($\eta\pi^0$), a) cl - distribution, b) t' - distribution, c) and d) mass($\eta\pi^0$) distribution

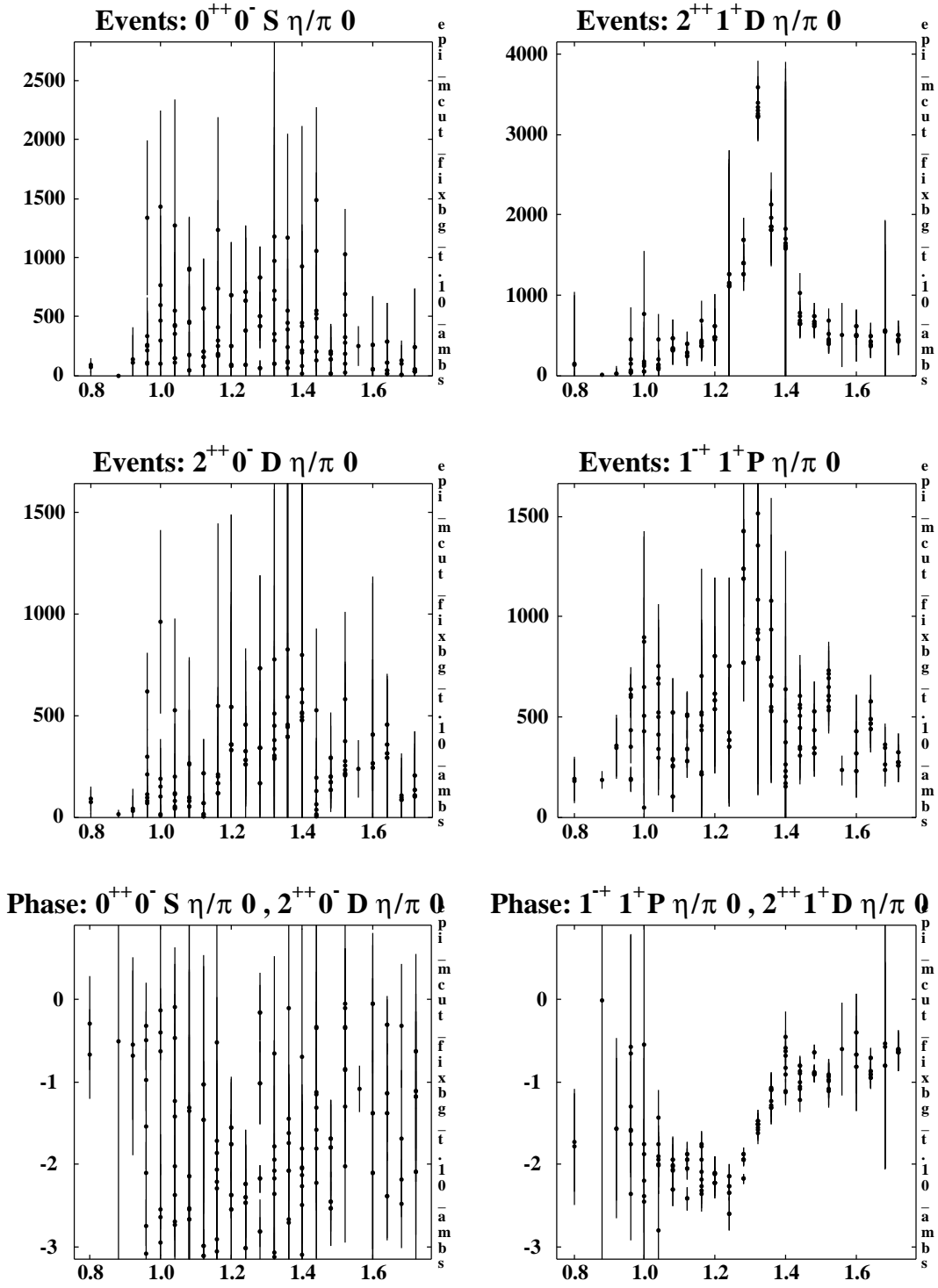


Figure 8: PWA of $\eta\pi^0$ system at fixed background and $|t'| > 0.1 \text{ GeV}^2$. Mass ($\eta\pi^0$) distributions of waves: a) S_0 , b) D_+ , c) D_0 , d) P_+ , e) phase (S_0, D_0), f) phase (D_+, P_+)

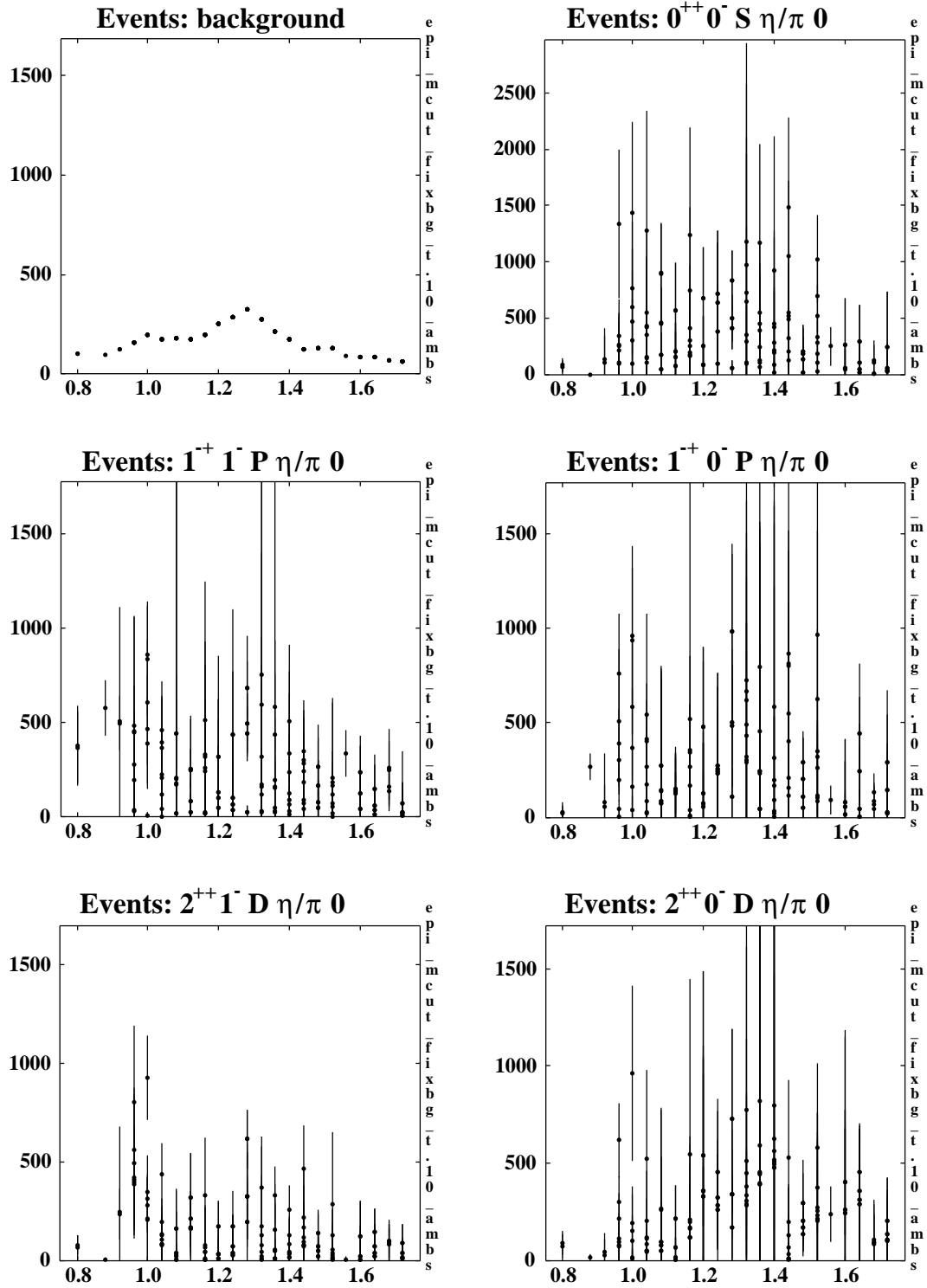


Figure 9: PWA of $\eta\pi^0$ system at fixed background and $|t'| > 0.1 GeV^2$. Mass ($\eta\pi^0$) distributions of waves: a) $Bcgr$, b) S_0 , c) P_- , d) P_0 , e) D_- , f) D_0

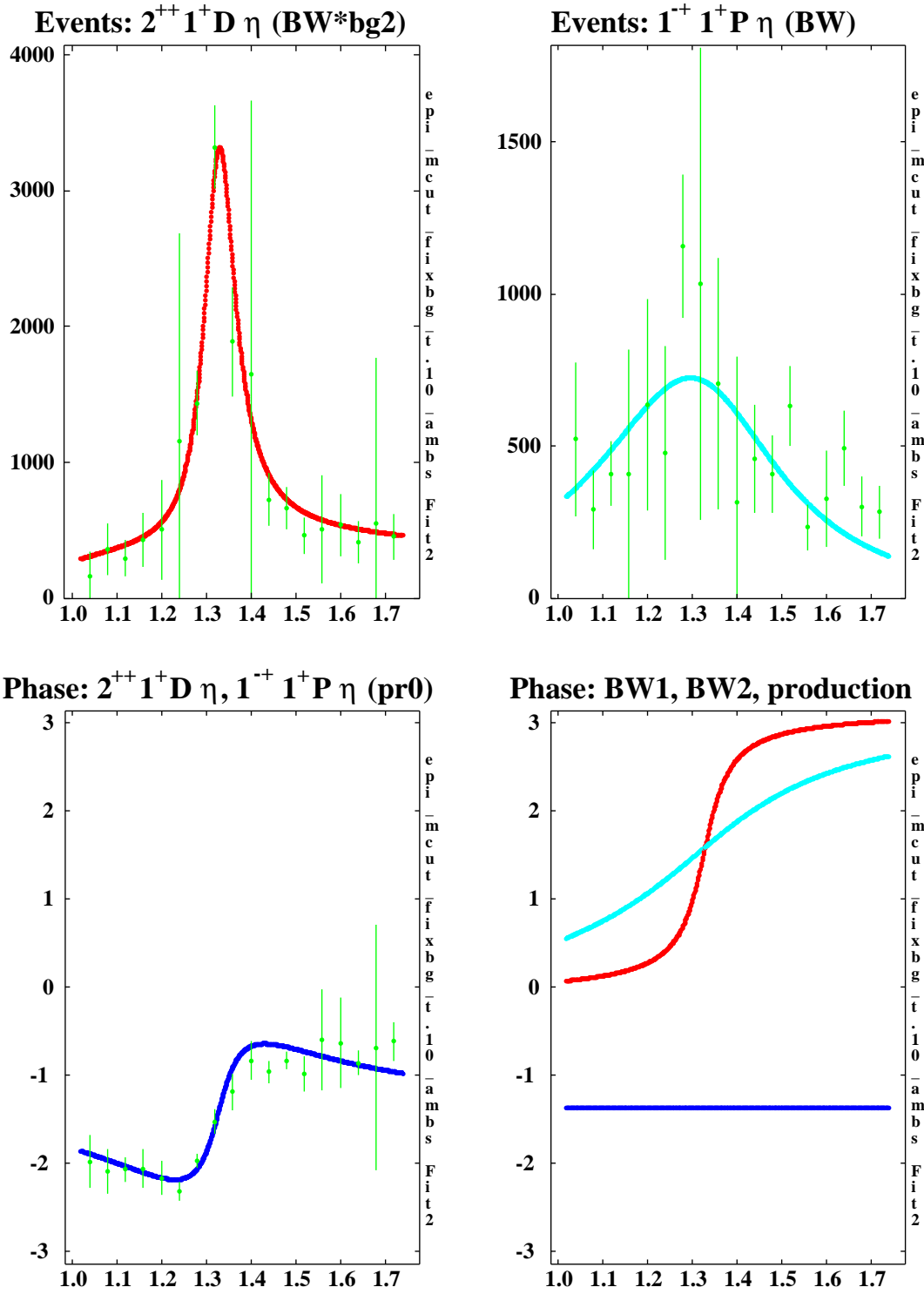


Figure 10: Mass dependent fit of two resonant waves D_+ and P_+ at $|t'| > 0.1 \text{ GeV}^2$. a) D_+ , b) P_+ , c) phase (D_+, P_+), d) BW and production phases